Freshwater Biology

Freshwater Biology (2015) doi:10.1111/fwb.12548

Extreme water quality degradation following a catastrophic forest fire

CLIFFORD N. DAHM*, ROXANNE I. CANDELARIA-LEY*, CHELSEA S. REALE†, JUSTIN K. REALE* AND DAVID J. VAN HORN*

Department of Biology, University of New Mexico, Albuquerque, NM, U.S.A.

†*Department of Earth and Planetary Sciences, University of New Mexico, Albuquerque, NM, U.S.A.*

SUMMARY

1. Global change is impacting the forests of the western United States through rising temperatures, earlier snowmelt, more rain and less snow, greater vapour pressure deficits in spring and autumn, forest dieback and increasing forest fire frequency and severity.
2. A catastrophic forest fire (Las Conchas fire) occurred in central NM, USA, in 2011 burning *c.* 634 km^2 with *c.* 46% of the fire being of severe or moderate intensity.
3. National Oceanic and Atmospheric Administration (NOAA) next-generation radar data (NEXRAD) were used to link precipitation events occurring in the burn scar to extreme water quality excursions observed in the Rio Grande. At four sites, *in situ* sensors captured the response of water temperature, specific conductance, pH, turbidity and dissolved oxygen to flood events following the fire.
4. Runoff from burn scars caused turbidity peaks (to 2500 NTU), dissolved oxygen sags (to 0.0 mg L^{-1}), pH sags (up to 0.75 units) and conductivity changes (both increases and decreases). These water quality excursions extended at least 50 km downstream, with significant implications for the ecosystem health of this crucial river that supplies water to cities and agriculture.
5. Sudden, dramatic changes to forested catchments from severe forest fires and forest dieback are very likely to be among the strongest impacts of global change on stream and river ecosystems throughout the western United States.

Keywords: continuous monitoring, dissolved oxygen, disturbance, forest fire, water quality

Introduction

The forests of the western United States (US) are changing rapidly. Rising temperatures enhance drought impacts, increasing tree mortality (Williams *et al*., 2012) and water limitation (Van Mantgem *et al*., 2009). The combination of earlier spring snowmelt (Knowles, Dettinger & Cayan, 2006), decreased winter precipitation (Seager *et al*., 2007; Seager, Tzanova & Nakamura, 2009) and greater vapour pressure deficit in the warm season (Williams *et al*., 2012) has substantially exacerbated stress on western US forests.

Forest fire is an important product of changing climate (Allen *et al*., 2010). Westerling *et al*. (2006) showed that large wildfire activity in the western United States increased suddenly and markedly in the mid-1980s. Wildfires now have higher frequencies, longer durations and longer seasons. The most impacted areas are mid-elevation forests with increased spring and summer temperatures and earlier spring snowmelt. These stresses also result in increased post-fire tree mortality and forest fire severity independent of fire intensity (Van Mantgem *et al*., 2013). Current and projected regional warming is seen as a major threat to human communities and forest ecosystems through increased wildfire activity (Westerling *et al*., 2006).

The south-western region of the western United States (southern California, Arizona, New Mexico) has been strongly affected by ongoing climate change and will be impacted by future climate change in the 21st century (Gutzler, 2013). A strong regional warming trend in air temperature (>1 °C) has enhanced evaporative losses

Correspondence: Clifford N. Dahm, Department of Biology, University of New Mexico, Albuquerque, NM 87131, U.S.A.
E-mail: cdahm@sevilleta.unm.edu

© 2015 John Wiley & Sons Ltd

and decreased mountain snowpacks. In addition, there is a recent trend towards aridity due to both decreasing precipitation in winter (the Hadley circulation moving poleward (Seager *et al.*, 2007)) and increasing evaporation associated with higher temperatures. Linear temperature projections using a mid-range projection of 21st century greenhouse gas emissions show an estimated 3.1 °C century^{-1} warming in winter and 3.8 °C century^{-1} warming in summer for this region of the US (Gutzler, 2013). Conditions that intensify fire regimes are occurring more frequently in the 21st century in the south-western United States and in New Mexico (NM) in particular. In the summer of 2011, low winter precipitation, early snowmelt of a reduced snowpack and high spring and summer temperatures set the stage for the largest forest fire in the recorded history of NM, the Las Conchas fire. This fire burned 63 370 hectares, but was surpassed in 2012 by the Whitewater-Baldy Complex fire in the Gila River Basin of south-western NM.

Wildfire effects on water quality are less commonly reported than effects on terrestrial ecosystems or the hydrology of burned catchments. Research on fire in forested catchments has focused on suspended sediment concentrations and exports with increases of up to three orders of magnitude above pre-fire values commonly reported (Shakesby & Doerr, 2006; Badia & Marti, 2008). More limited data are available on the effects of forest fires on the export of nutrients, dissolved organic carbon and trace elements (Smith *et al.*, 2011). An important observation from these limited studies is that the export of these constituents after forest fires is increased (up to more than two orders of magnitude above background) with many constituents linked to the increases in suspended sediments. The vast majority of these studies are based on measurements made on grab samples from burned catchments with limited spatial and temporal coverage of forest fire impacts. Continuous measurements of water quality in streams and rivers draining catchments impacted by forest fires are rare.

A network of continuously measuring water quality sensors (sondes) has been deployed in the Rio Grande of central NM since 2006. This network lies immediately downstream of major catchments burned by the 2011 Las Conchas fire. Water quality impacts on the Rio Grande immediately after the Las Conchas fire were determined by comparing long-term data collected from the network before and after the event. This study focuses on immediate water quality responses to post-fire flow events deriving from burned catchments upstream of the sensor network. Specific goals of the study are to (i) examine water quality responses (temperature, specific conductance, pH, dissolved oxygen and turbidity) from the first few storms after a major, high severity forest fire, (ii) follow the propagation of forest fire effects on water quality through a network of stations along a major river and (iii) document the role of monsoonal thunderstorms on the transport of fire scar material into the fluvial network and observe subsequent effects of these storms on water quality.

Site description

Research was carried out in the Rio Grande in central NM, U.S.A. (Fig. 1). The Rio Grande is a major dryland river and the fifth-longest river (2830 km) in the United States (Fig. 1a). The study region, the Middle Rio Grande (MRG), runs through central NM for *c.* 290 km, from the Otowi streamflow gauge (USGS 08313000) above Cochiti Reservoir (Fig. 1b) to Elephant Butte Reservoir. The MRG has recently been tapped as a drinking water source for Albuquerque (*c.* 550 000 residents) and Santa Fe (*c.* 68 000 residents) via surface water diversions, to supplement and replenish groundwater resources in the basin. The MRG flows through a rift valley containing deep sedimentary deposits (> 10 km) and with extensive levees to protect urban centres along the river. Dominant trees within the floodplain are native Rio Grande cottonwoods (*Populus deltoides* subspecies *wislizenii*) and Goodding's willows (*Salix gooddingii*) and non-native salt cedars (*Tamarix* spp.) and Russian olives (*Elaeagnus angustifolia*). The catchment area for the MRG Basin is *c.* 39 220 km^2 (Dahm *et al.*, 2002).

Historically, the MRG was a sinuous and braided snowmelt-dominated ecosystem with an extensive floodplain that had a tendency to aggrade sediment and was prone to extensive seasonal flooding (Molles *et al.*, 1998). Today, the MRG is a human-dominated and highly engineered system with discharge strongly controlled by reservoir releases (Bestgen & Platania, 1991). Within the MRG, three major dams have been constructed since 1948 (Jemez Canyon (1953), Galisteo (1970), Cochiti (1973)) for flood and sediment control. Since 2002, Jemez Canyon Dam has operated as a pass-through facility, with partially open gates, and stores water only temporarily during extreme flooding. Agricultural diversions on the MRG also reduce flows downstream (Dudley & Platania, 2007). Pulses of higher flows in the MRG occur from inflows from intermittent rivers. These flows are of short duration and derive from intense monsoonal thunderstorms that commonly occur in July and August.

© 2015 John Wiley & Sons Ltd, *Freshwater Biology*, doi: 10.1111/fwb.12548

These monsoonal thunderstorms also contribute appreciable quantities of transported sediment. From a general water quality perspective, average annual water temperature, specific conductance and turbidity increase longitudinally along the MRG from Cochiti to Elephant Butte reservoirs (Turner & Edwards, 2012).

The Las Conchas fire began on 26 June 2011 in the Jemez Mountains of central NM and was declared 100% contained on 3 August 2011 (Fig. 1d). In total, the fire burned 63,370 hectares of woodland, high montane grassland and meadows in the Jemez Mountains and suppression costs exceeded $40.9 million. Burn severity within the burn perimeter was *c.* 20% high severity, 26% moderate severity, 39% low severity and the rest unburned (Fig. 1d). Much of the forested headwaters of the Jemez River, a major tributary to the Rio Grande (Fig. 1b), was burned along with the headwaters of numerous smaller catchments that discharge directly into the Rio Grande or the Rio Chama in central NM.

Many tributaries to the Rio Grande that were impacted by the Las Conchas fire had not experienced extreme flooding for many years, and consequently, large amounts of stored sediments were easily entrained after the fire by runoff from the denuded landscape (Pelletier & Orem, 2014). Similarly, other recent forest fires prior to the Las Conchas fire and subsequent floods in the Jemez Mountains have increased sediment and debris loads in the Rio Grande and in many of its tributaries (Veenhuis, 2002; Lavine *et al.*, 2006; Malmon *et al.*, 2007). The topography of the region is generally moderately steep to very steep within the burned area. The tuff and pumice-derived soils are productive, but have very high erosion potentials when vegetation is absent due to low bulk density of the extrusive volcanic parent material. In addition, fire-induced water repellency has been noted for soils that are derived from pumice, and *c.* 14 164 ha (22.4%) of the burn area had water-repellent soils as defined by DeBano (1981), although the effects of fire-induced hydrophobicity on runoff and erosion are strongly debated (DeBano, 2000). Drought, which lasted through most of July and induced soil moisture deficiencies, may have increased the surficial hydrologic and geomorphic responses to fire-induced water repellency within the Las Conchas burn scar (Walsh *et al.*, 1994). In summary, the Las Conchas fire moderately or severely burned a large area resulting in extreme examples of hillslope runoff and floodplain erosion from these surfaces throughout the burn scar region.

Burn scar runoff that entered the Rio Chama or the Rio Grande above Cochiti Reservoir was retained in Cochiti Reservoir with a single exception during the study period. Cochiti Reservoir is managed by the U.S. Army Corps of Engineers and is authorised for flood control, sediment control and a permanent conservation pool. The median water residence times in the reservoir during July and August 2011 were 0.7 and 0.9 months, respectively. The outlet to the reservoir is hypolimnetic release. Subcatchments that flow directly from the burn scar to the Rio Grande below Cochiti Reservoir are strong candidates for producing water quality impacts on the MRG (Fig. 1c). The three primary subcatchments that have headwaters in the burn scar are Peralta Canyon, Santo Domingo Canyon and an unnamed canyon immediately west of Santo Domingo Canyon, with Peralta Canyon being the most strongly impacted subcatchment.

The Peralta Canyon subcatchment covers *c.* 117 km^2 and ranges in altitude from 1615 to 2743 metres above mean sea level (U.S. Army Corps of Engineers, 2012). About 72 km^2 (62%) of the catchment burned during the Las Conchas fire in 2011 (Fig. 1c). Burn severity within the catchment was 25% high severity, 42% moderate severity and 33% low severity. Ownership of the Peralta Canyon subcatchment includes the Pueblo de Cochiti, the Bureau of Land Management and the Santa Fe National Forest. Prior to the fire, the headwaters area was a densely forested basin that changed from mixed conifer into pinyon-juniper woodland with decreasing elevation. Because of the severity of the Las Conchas fire, the hydrology of Peralta Canyon was strongly altered by reductions in infiltration, increases in the rate of runoff and reductions in the lag time between peak precipitation and peak runoff (U.S. Army Corps of Engineers, 2012).

The distance between the centre of the burn area in Peralta Canyon and the confluence with the Rio Grande is 17.3 km (Fig. 1b). The distance from the confluence of Peralta Canyon with the Rio Grande and the San Felipe gauge is 21.6 km. The distance from the San Felipe gauge to the first sonde location at the 550 Bridge is 20.1 km. Distances from the 550 Bridge sonde location to the other sondes at Alameda, Rio Bravo and I-25 along the MRG are 18.8 km, 41.2 km and 50.4 km, respectively. There are no reservoirs along this reach of the Rio Grande.

Methods

Validated streamflow data for July and August 2011 were collected from five U.S. Geological Survey (USGS) gauges (Embudo - 08279500, Otowi - 08313000, Cochiti - 08317400, San Felipe - 08319000, and Central - 08330000)

© 2015 John Wiley & Sons Ltd,

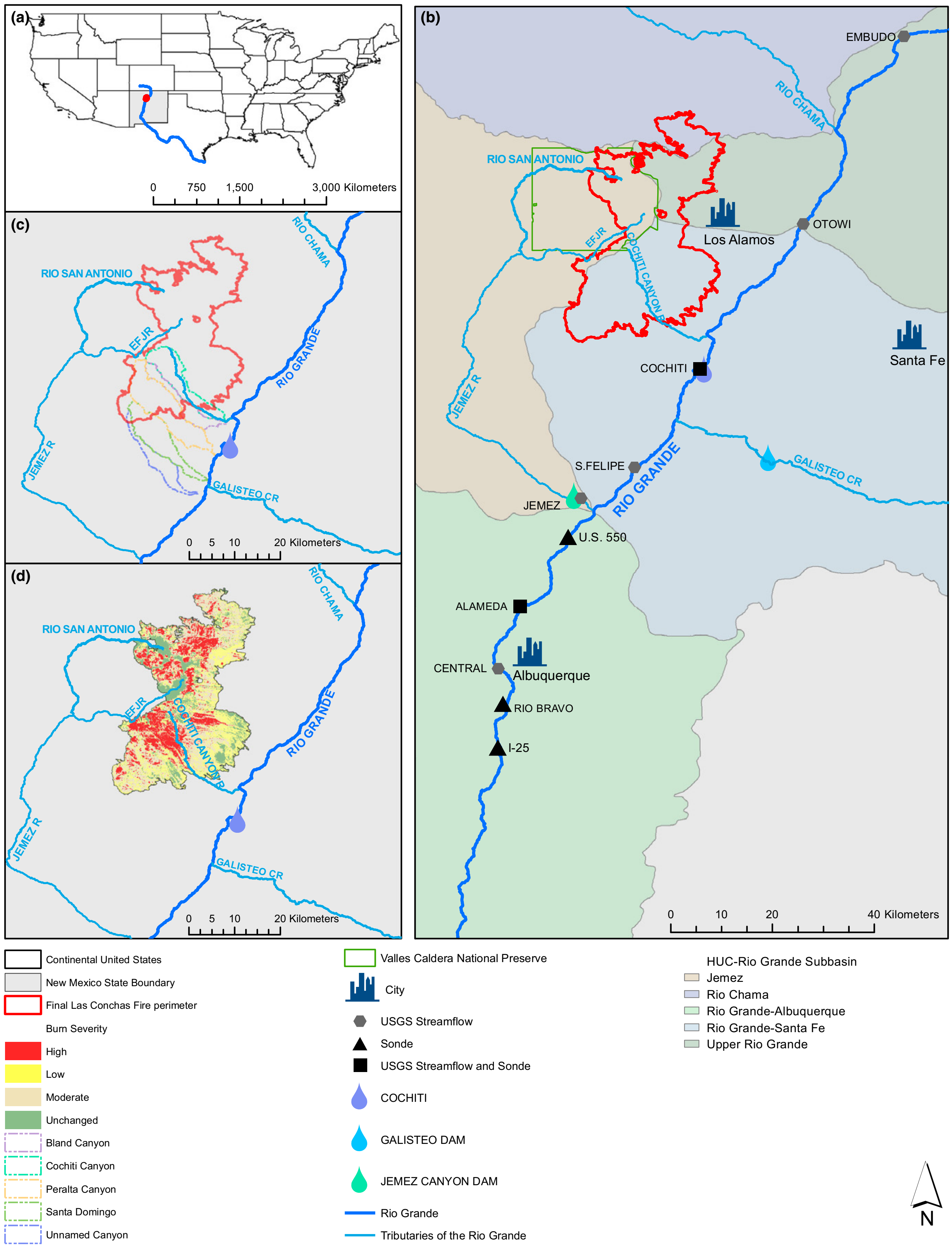
(a)
0 750 1,500 3,000 Kilometers
(b)
EMBUDO
RIO CHAMA
RIO SAN ANTONIO
EFJR
COCHITI CANYON R
Los Alamos
OTOWI
Santa Fe
COCHITI
JEMEZ R
GALISTEO CR
S.FELIPE
RIO GRANDE
JEMEZ
U.S. 550
ALAMEDA
CENTRAL
Albuquerque
RIO BRAVO
I-25
0 10 20 40 Kilometers
(c)
RIO CHAMA
RIO SAN ANTONIO
EFJR
RIO GRANDE
JEMEZ R
GALISTEO CR
0 5 10 20 Kilometers
(d)
RIO CHAMA
RIO SAN ANTONIO
EFJR
COCHITI CANYON R
RIO GRANDE
JEMEZ R
GALISTEO CR
0 5 10 20 Kilometers
Continental United States
New Mexico State Boundary
Final Las Conchas Fire perimeter
Burn Severity
High
Low
Moderate
Unchanged
Bland Canyon
Cochiti Canyon
Peralta Canyon
Santa Domingo
Unnamed Canyon
Valles Caldera National Preserve
City
USGS Streamflow
Sonde
USGS Streamflow and Sonde
COCHITI
GALISTEO DAM
JEMEZ CANYON DAM
Rio Grande
Tributaries of the Rio Grande
HUC-Rio Grande Subbasin
Jemez
Rio Chama
Rio Grande-Albuquerque
Rio Grande-Santa Fe
Upper Rio Grande
N

Fig. 1 Maps showing the Rio Grande, the study area in the Middle Rio Grande in central New Mexico, eastward draining catchments to the Rio Grande from the Las Conchas burn area and a burn severity map for the Las Conchas fire. Panel (a) shows the location of the Rio Grande and the Las Conchas forest fire in north-central New Mexico. Panel (b) shows the USGS streamflow gauges, the four water quality sondes, major tributaries of the Rio Grande, the perimeter of the Las Conchas fire, key landmarks and the major hydrologic unit codes (HUCs) for this section of the Rio Grande. Panel (c) shows catchments that discharge directly into the Rio Grande that contain headwaters in the burn scar area. Panel (d) maps the burn severity of the Las Conchas fire.

on the Rio Grande within and outside the Las Conchas burn zone (Fig. 1). In addition, the USGS gauge on the Jemez River downstream of Jemez Canyon Dam (08328950) near the confluence with the Rio Grande was included in the assessment to determine whether flows from this tributary contributed to water quality degradation. Discharge estimates for major flash floods from Peralta Canyon and Cochiti Canyon were obtained from estimates of stage, cross-sectional area and velocity by the New Mexico Environmental Department ((NMED; D. Englert & R. Ford-Schmid, unpublished data).

Water quality (WQ) has been monitored by our group along the main stem of the Rio Grande in central NM from 2006 to 2011. Dissolved oxygen (DO – rapid pulse polarographic probe), temperature, specific conductance, pH and turbidity data were collected at 15-min intervals at four water quality monitoring sites along the Albuquerque reach of the Rio Grande (Fig. 1b). These sites are the US 550 Bridge (Lat. 35.322091, Long. -106.557463), the Alameda Bridge (Lat. 35.196945, Long. -106.642502), the Rio Bravo Bridge (Lat. 35.027263, Long. -106.672669) and the I-25 Bridge (Lat. 34.949956, Long. -106.68176). Water quality data were obtained using Yellow Springs Instruments (YSI) 6920 multiparameter sondes (YSI Inc./Xylem Inc., Yellow Springs, OH, U.S.A.). This project also used additional WQ data (dissolved oxygen - optical DO probe, temperature, specific conductance and turbidity) collected by the USGS in conjunction with the Albuquerque Metropolitan Arroyo Flood Control Authority (AMAFCA) at a water quality monitoring site at the US 550 Bridge, *c.* 50 m from the sonde deployed by our group. The USGS WQ data were collected continuously every 5 min using an In-situ TROLL 9000 Pro XP sonde (In-situ Inc., Fort Collins, CO, U.S.A.). The USGS record assisted in the validation of our sonde data, provided additional turbidity data beyond the detection limits of the YSI sondes and supplemented gaps in our WQ record at US 550.

Site visits were made at 2–4 week intervals to clean and calibrate the sondes following USGS standard operating procedures (Wagner *et al.*, 2006). Briefly, equipment was cleaned and calibrated using laboratory-quality conductivity, pH and turbidity standards. Dissolved oxygen was calibrated in water-saturated air. Thermistors for temperature measurements were stable and did not require routine calibration. Readings before cleaning, after cleaning and after calibration were taken alongside a laboratory-calibrated comparison sonde to determine any fouling drift and/or calibration drift.

Turbidity (measured by the USGS In-situ TROLL 9000 Pro XP sonde with maximum turbidity capability to 2000 NTU and with the YSI turbidity probe with a maximum reading of 1000 NTU) dropped below pre-storm baseline values to a reading of *c.* 0 NTU during flow pulses between August 18 and 23 (Figs. 5 and 6). This occurred when DO values were very low or zero, and the river was choked with black ash and charcoal (black carbon) from the burn scar. Laboratory trials using a solution containing suspended crushed charcoal produced readings of 0 NTU because large loads of black carbon absorbed all light in the detection cell, thereby simulating the conditions of no light scattering under which the probe is calibrated as 0 NTU.

Water quality data were validated using Aquarius Workstation 3.3 (Aquatic Informatics, Vancouver, British Columbia, Canada) and graded according to USGS ratings for accuracy (Wagner *et al.*, 2006). Suspect data were identified, and the possible causes of low quality data (i.e. instrument fouling, exposure to air, low voltage) were documented. Outliers, out of range data and invalidated data were removed. Data were corrected for any fouling drift and calibration drift. Approved WQ and discharge records for July and August 2011 were evaluated for their responses to precipitation events within the catchment with a particular focus on precipitation events occurring upon the burn scar from the Las Conchas fire. River flow and precipitation data were analysed along with the WQ parameters to determine when excursions due to runoff from the fire scar might occur at the downstream sonde locations.

Daily (24 h) archived Next Generation Weather Radar (NEXRAD) data were gathered for July and August 2011. NEXRAD is a multisensor Doppler weather radar network developed by the U.S. National Oceanic and Atmospheric Administration (NOAA) and implemented and maintained by the U.S. National Weather Service (NWS). NEXRAD detects precipitation using ground-

© 2015 John Wiley & Sons Ltd, doi: 10.1111/fwb.12548

based radar. The downloaded NEXRAD data are represented by equidistant points 4 km apart. Each point can be considered a centroid representing the amount of precipitation that fell within a *c.* 16 km^2 cell.

ArcGIS 10.0 (ESRI, Redlands, CA, USA) was used to create a grid system for analysis of precipitation that fell within a designated boundary. Each daily NEXRAD data set was clipped to the boundary of the final Las Conchas fire perimeter (Fig. 1b–d). Thiessen polygons (proximal zones) were created for each daily data set. These zones represent full areas where any location within the zone is closer to its associated input point than to any other input point. The gridded precipitation data and boundary layers allowed segregation of precipitation within the defined area of the fire perimeter and the estimation of daily precipitation for the burn area.

Results

No storm-related pulses were observed during July and August 2011 at the most upstream gauge above the confluence with the Rio Chama (Embudo gauge, Fig. 2). Downstream of the Embudo gauge numerous monsoonal precipitation events resulted in flow and water quality excursions. The Rio Chama enters the Rio Grande downstream of Embudo carrying tributary inputs and storm flows from the northern portion of the Jemez Mountains (including catchments within the Las Conchas burn scar), other contributing ungauged intermittent river basins and releases from El Vado Reservoir and Abiquiu Reservoir, all of which affect flows on the Rio Chama (Fig. 1b). Releases from these dams varied greatly during this study as downstream water delivery obligations were fulfilled and recreational flows were implemented. The combined Rio Chama and mainstem Rio Grande flows at the Otowi gauge (Fig. 1b) showed diurnal variability, storm pulses and reservoir releases during the 2-month study period (Fig. 2 – Otowi gauge).

Between the Otowi gauge and Cochiti Reservoir, several large floods caused by runoff from the burn scar occurred in high gradient tributaries that flow through canyons to reach the Rio Grande above the Cochiti Reservoir. Although these tributaries are ungauged and the flows are intermittent, NMED estimated that discharge during one event in Cochiti Canyon (Fig. 1c) on 22 August 2011 reached *c.* 540 m^3 s^{-1} (D. Englert & R. Ford-Schmid, unpublished data). Precipitation during storm events falling upon burn scar material, particularly in severely and moderately burned sectors, mobilises ash, charcoal and soil that moves into and through the stream and river network (Fig. 3). Floodwater storage in Cochiti Reservoir and controlled releases from the dam removed the effects of most of these upstream storm events from the hydrographs below Cochiti Dam with the exception of a water quality pulse observed immediately below Cochiti reservoir on August 22 and 23, likely related to the large Cochiti Canyon flood (Fig. S1). The pulse flows observed in the MRG were primarily from intermittent rivers flowing through canyons,

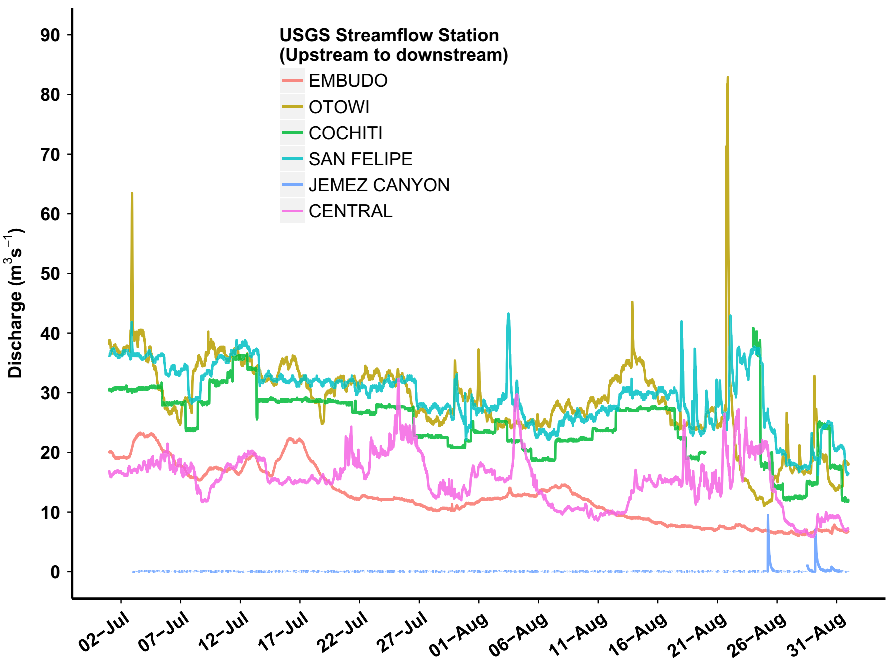

Fig. 2 Hydrographs for July and August 2011 for gauges on the Middle Rio Grande plus the Jemez Canyon gauge on the Jemez River. The Embudo gauge is above the confluence with the Rio Chama. Discharge pulses reflect runoff from monsoonal thunderstorms from catchments within the Middle Rio Grande.

Fig. 3 Photographs showing that initial flood events generated by monsoonal thunderstorms upon the Las Conchas burn scar mobilised large quantities of organic matter and transported it to the MRG. Panel (a) shows the transport of ash and charcoal from a severely burned stand of trees down into a meadow within the Valles Caldera National Preserve. Panel (b) is of the first flood flow after the Las Conchas fire in late July from first-order Indio Creek in the Valles Caldera National Preserve. The erosive energy of the flood, the black colour of the water and strong overbanking of this small stream are apparent. Panel (c) shows water collected from Indios Creek before the flash flood and during the first flash flood after the Las Conchas fire. The black carbon in transport in the flood waters is clearly seen. Panel (d) shows a flash flood in the intermittent river in Cochiti Canyon on Cochiti Pueblo on 22 August 2011. Panel (e) shows the confluence with the Rio Grande downstream of where the intermittent rivers flowing through Bland Canyon and Cochiti Canyon come together and then join the Rio Grande. This photograph was taken the day after a major flash flood from the Las Conchas burn scar in August 2011. Panel (f) shows the Rio San Antonio in late July 2011 after the first flash flood from the Las Conchas burn scar reached this third-order stream. Note the large amount of floated organic debris in transport by the stream.

predominantly Peralta Canyon, that enter the Rio Grande below Cochiti Dam causing increases in river discharge in early and late August (Fig. 2 – San Felipe gauge). These flash floods resulted from runoff events on the fire burn scar and were recorded first at the San Felipe gauge and then propagated downstream to the Albuquerque gauge at Central (Fig. 2). Although numerous flow events also occurred in the upstream portions of the Jemez River during July and August 2011, only a few small pulses in late August reach the lower Jemez River and were recorded below the Jemez Canyon Dam, near the confluence with the Rio Grande (Fig. 2 – Jemez gauge). The Jemez River was not a significant source of fire-related storm water pulses to the Rio Grande during July and August 2011 (Fig. 2).

We examined DO at our upstream monitoring station (US 550 Bridge) for July and August for 3 years prior (2007, 2008 and 2010) to the Las Conchas fire and for 2011 immediately after the Las Conchas fire to look for fire effects (Fig. 4). DO data from July and August in

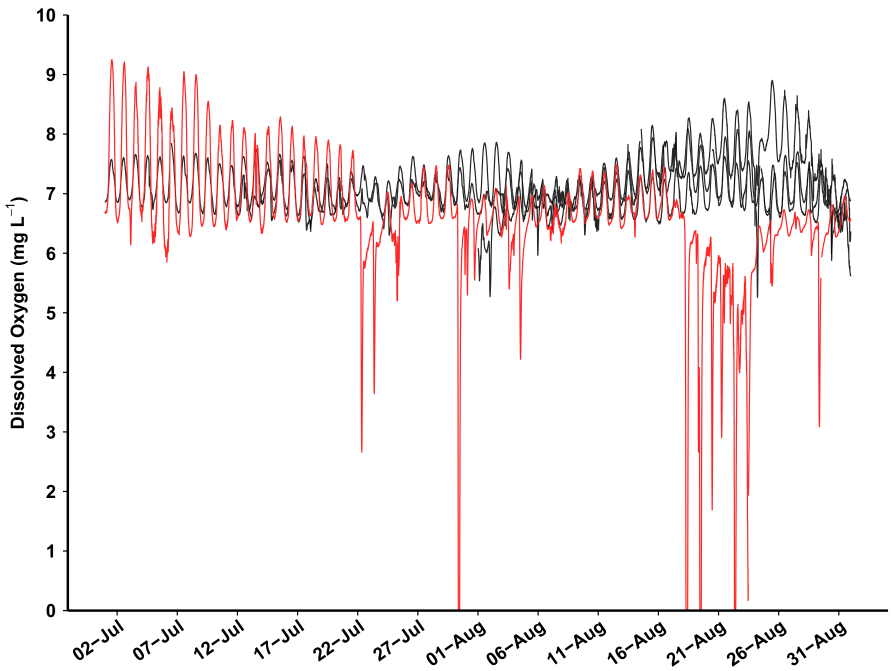

Fig. 4 Continuous dissolved oxygen concentrations in the Rio Grande in July and August at the US 550 Bridge site in 2007, 2008 and 2010 in black (pre-fire) and for 2011 in red (post-fire).

Table 1 Dissolved oxygen sags measured during July and August 2011 at the US 550 Bridge site. Change in dissolved oxygen indicates the difference in concentration from the beginning of the sag to the minima

Date	Dissolved oxygen minima (mg L^{-1})	Change in dissolved oxygen (mg L^{-1})
7/22/2011	2.66	3.67
7/23/2011	3.64	2.71
7/30/2011	0.00	6.61
8/4/2011	4.22	2.31
8/18/2011	0.00	6.03
8/19/2011	0.00	6.13
8/20/2011	1.69	4.30
8/21/2011	2.92	2.72
8/22/2011	0.00	5.72
8/23/2011	0.17	5.23
8/29/2011	3.09	3.11

2007, 2008 and 2010 showed no excursions below 5 mg L^{-1} with only a few instances of values below 6 mg L^{-1} (Fig. 4). In strong contrast to 2007, 2008 and 2010, 15 DO sags below 6 mg L^{-1} occurred during July and August 2011 with four events reaching anoxia (Fig. 4 – red line, Table 1).

From 17–25 August 2011 was a period with numerous and severe WQ excursions during strong monsoonal activity in the burn scar region (Figs. 5 and 6). Concurrent with each of the DO sags was an increase in specific conductance at US 550 Bridge, the largest of which nearly doubled values from *c.* 270 μS cm^{-1} to *c.* 500 μS cm^{-1} and sags in pH of up to *c.* 0.75 pH units (Fig. 5). During each of these excursions in WQ, turbidity began to increase as DO declined and conductivity spiked. However, measured turbidity fell below pre-storm baseline values due to spurious readings of ~0 NTU as the pulses continued on August 18, 19, 22 and 23 (Fig. 5) because of interference by black carbon and extremely high turbidity levels.

Water quality parameters at the downstream Alameda site (Fig. 6) for 17–25 August 2011 displayed similar patterns to those observed at US 550, with two exceptions. We observed a DO sag to *c.* 2.5 mg L^{-1}, a specific conductance sag of *c.* 75 μS cm^{-1}, a turbidity spike of *c.* 350 NTU and a small pH sag and spike late on August 17 and early on August 18 that were not present at the US 550 site. A similar event with similar types of WQ responses was observed on August 21 that also was not seen at the US 550 site. Both events resulted from flows from the Albuquerque North Floodway Channel (peak flows to *c.* 35.4 and 21.2 m^3 s^{-1}), which conveys stormwater runoff from a large portion of the City of Albuquerque and discharges into the Rio Grande 3.2 km above the Alameda site. Similar DO sags linked to urban runoff have been

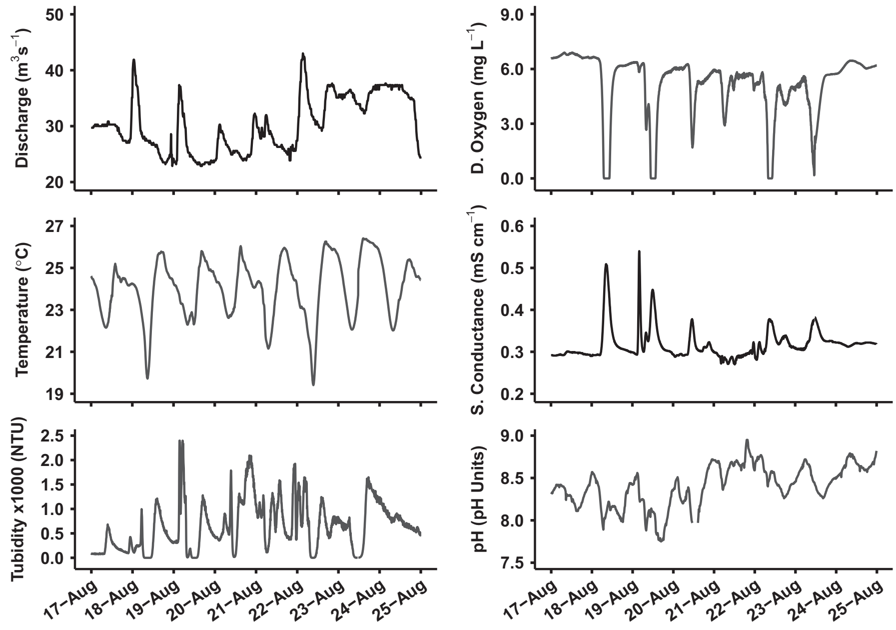

Fig. 5 Water quality parameters (temperature, turbidity, dissolved oxygen, specific conductance and pH) and discharge at the US 550 Bridge site from 17 to 25 August 2011.

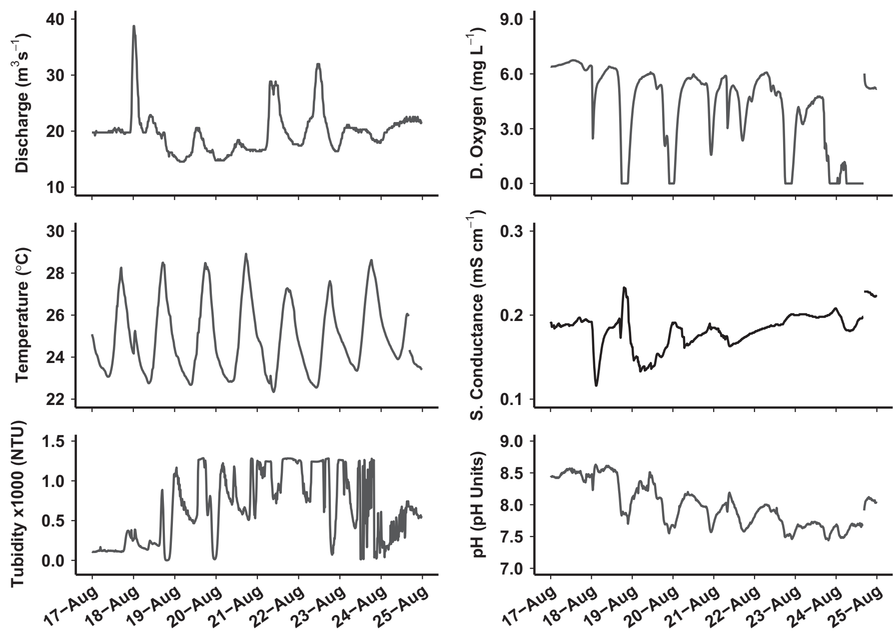

Fig. 6 Water quality parameters (temperature, turbidity, dissolved oxygen, specific conductance, and pH) and discharge at the Alameda Bridge site from 17 to 25 August 2011.

observed at this site in previous years. Therefore, WQ responded almost immediately to increases in discharge of Albuquerque urban runoff. Conversely, peak WQ fluctuations from discharge events carrying burn scar materials from the Las Conchas fire occurred *c.* 8–10 h after initial increases in river discharge. The sags and peaks in the various water quality parameters that occurred at both sites were both attenuated and accentuated at the Alameda site as compared to those that occurred at the upstream US 550 site. For example, DO at Alameda remained anoxic for longer periods of time, but the changes in specific conductance and pH were muted compared to the US 550 site. Finally, turbidity at Alameda was measured with an YSI sonde with maximum detection limits of 1000 NTU, and the detection limits were exceeded much of the time between August 19 and August 23 with periodic collapses to 0 NTU when black carbon concentrations were extremely high. Comparisons of absolute turbidity values between the two sites are difficult because of the use of two different types of turbidity probes with differing abilities to measure high turbidities.

© 2015 John Wiley & Sons Ltd, *Freshwater Biology*, doi: 10.1111/fwb.12548

Data for DO from all four WQ stations were used to follow the propagation downstream for several of the most severe fire scar-related runoff events along 50.4 km of river (Fig. 7). Travel time from the upstream to downstream site was *c.* 28 h. During the four severe events that occurred during the last 2 weeks of August, DO data were unavailable at the site furthest downstream (I-25) for the first two events due to probe malfunction. However, three of these sags decreased the DO in the MRG to *c.* 0.0 mg L^{-1} for at least 41.2 km downstream of our uppermost site (US 550 to Rio Bravo), while DO during one of these sags returned to *c.* 1.0 mg L^{-1} by the downstream site (Rio Bravo). Data for the last two events of August at the furthest downstream site showed attenuation to *c.* 1.0 and *c.* 3.0 mg L^{-1}, respectively. Severe DO sags associated with flow events propagating from the Las Conchas burn scar thus extended over large distances along the main stem of the MRG.

Spatially detailed analyses of monsoonal thunderstorms within the burn scar, stream discharge and DO concentrations showed that storm pulses caused DO sags downstream. Four distinct time periods during the monsoon season of 2011 were found when monsoonal precipitation waxed and waned (Fig. 8). Minimal precipitation occurred over the burn scar for the first period from July 1 through July 19 with no observed storm pulses or DO excursions along the MRG. In the second period from July 20 through August 7, multiple precipitation events occurred over the burn scar that increased river discharge. During this period, five DO sags were observed at US 550, with one event resulting in anoxia on July 30. Analysis of the third distinct period from August 8 through the August 17 revealed minimal precipitation on the burn scar with a generally stable hydrograph and no DO sags. Multiple precipitation events occurred within the burn scar during the fourth period from August 18 through August 31, including the largest precipitation total of *c.* 21 mm on August 22. These frequent and sometimes intense precipitation events caused significant increases in discharge and seven DO sags, with two resulting in hypoxia (<2 mg L^{-1}) and three resulting in anoxia.

Discussion

Climatological and meteorological conditions

Both climatological and meteorological conditions contributed to the size and severity of the Las Conchas fire in 2011. Interannual climate variability in the southwestern United States is strongly linked to the North American Monsoon in summer and the El Niño Southern Oscillation (ENSO) phenomenon in autumn, winter and spring (Sheppard *et al.*, 2002; Touchan *et al.*, 2011). Winter snowpack and spring runoff of NM mountain streams are strongly affected by the status of the ENSO phenomenon with greater snowpack and spring runoff during El Niño years and with lower snowpack and spring runoff during La Niña years (Molles & Dahm, 1990). The autumn, winter and spring period of 2011

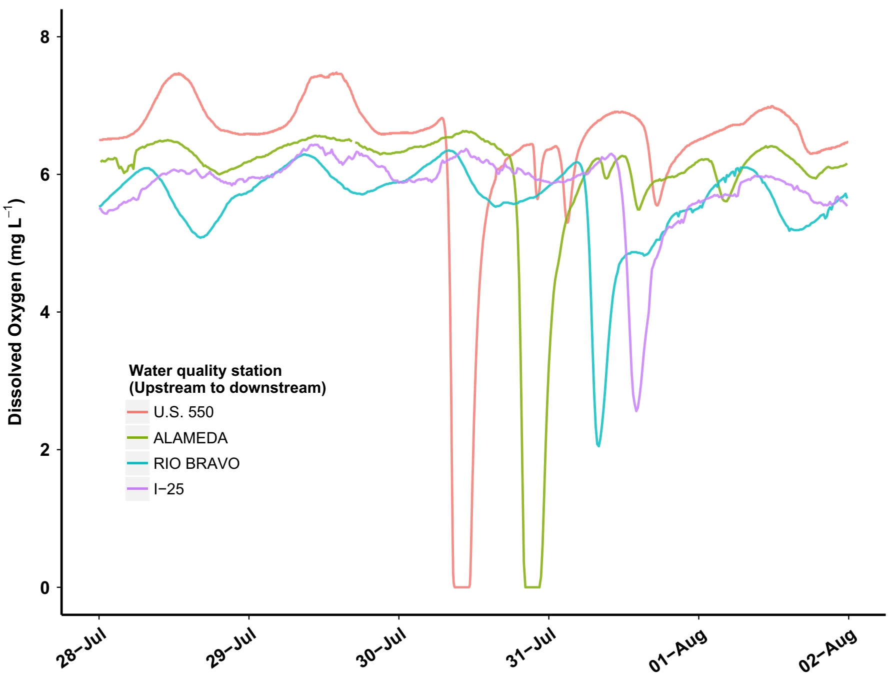

Fig. 7 Propagation of a dissolved oxygen sag along the Rio Grande from the upstream US 550 Bridge site to the Alameda, Rio Bravo, and I-25 bridge downstream sites on 30 and 31 July 2011 after monsoonal thunderstorm runoff at the Las Conchas burn scar. The distance between the US 550 Bridge site to the I-25 Bridge site is 50.4 km.

© 2015 John Wiley & Sons Ltd, *Freshwater Biology*, doi: 10.1111/fwb.12548

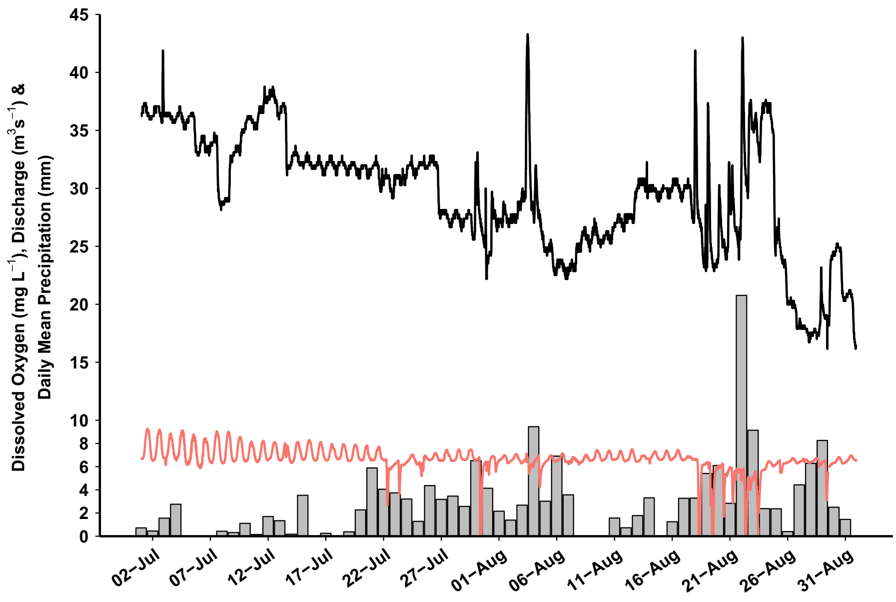

Fig. 8 Discharge, dissolved oxygen concentrations and daily mean precipitation on the Las Conchas burn scar for July and August 2011. Note the general concordance between strong monsoonal precipitation on the burn scar with discharge pulses and dissolved oxygen sags. The black line is discharge at the San Felipe gauge, the red line is the dissolved oxygen concentration at the US 550 Bridge, and the grey bars are estimated daily precipitation values in mm on the burn scar.

was a strong La Niña year with minimal snowpack and low runoff throughout the MRG Basin. In addition, the spring of 2011 had mild temperatures and low humidity. The months before the Las Conchas fire were both extremely dry (25–50% of normal for the Jemez Mountain catchment from October 2010 to May 2011) and unusually warm (8th warmest March through May in 117 year record for NM) resulting in conditions conducive to forest fires.

The trend towards smaller snowpacks, earlier and diminished snowmelt, warmer spring and summer temperatures and decreased spring and summer soil moisture content provides ideal conditions for large high-intensity forest fires with subsequent impacts to stream and rivers in the forested catchments of the south-western United States. Frequent low intensity surface fires in the Jemez Mountains with 5–25 year return intervals dominated pre-1900, but have been supplanted by larger, higher intensity stand-replacing fires in recent decades due to anthropogenic fire suppression and the build-up of woody fuels (Allen, 2001). These trends, and our data, suggest that severe water quality impacts from high-intensity fire will also increase in frequency in forested catchments of the south-western United States.

Water quality impacts

Overland flow, flooding and erosion are common in catchments after high-intensity, stand-replacing fires and subsequent rains (Shakesby & Doerr, 2006), resulting in strong WQ responses (Gresswell, 1999; Smith *et al*., 2011; Verkaik *et al*., 2013). The continuous water quality data set available for years prior to, during and after the Las Conchas fire in this study provides new added insights with good temporal resolution for several interrelated WQ parameters. As documented in other stream ecosystems (DeBano, 2000; Shakesby & Doerr, 2006; Smith *et al*., 2011), fire inputs markedly increased suspended sediment loads in the MRG, routinely exceeding the detection limits for turbidity for the instruments deployed in the river. Although discrete sampling has shown that forest fires typically transport large quantities of ash and debris, our data provide less frequently reported continuous turbidity values (NTU) useful for surface water treatment intake facilities (Smith *et al*., 2011). In fact, the water intake for the City of Albuquerque was shut down for 66 days in the late summer and early autumn of 2011 because of high turbidity in the Rio Grande. We also show the downstream movement of large quantities of black carbon; however, additional research is needed to understand the impact of these events on the river ecosystem. Interestingly, these black carbon pulses were observed as turbidity sags rather than pulses as they inhibited the ability of the sensors to record turbidity. This limitation should be considered when using similar instruments to investigate fire effects in other systems.

This is the first study to our knowledge to collect continuous specific conductance and pH data following a fire. The increases in conductivity during the first few smaller pulses of burn scar materials are likely a result of the solubilisation of ions from fresh ash, a process observed from grab sampling after the addition of fire

© 2015 John Wiley & Sons Ltd, *Freshwater Biology*, doi: 10.1111/fwb.12548

ash to another stream in NM (Earl & Blinn, 2003) as well as in other fire-impacted streams (Hall & Lombardozzi, 2008). However, larger pulses later in the summer had lower specific conductance than pre-pulse values, likely as a result of the removal of soluble constituents in the initial floods and dilution of background concentrations by the later stronger discharge pulses. The pH sags in association with pulses of water from the Las Conchas fire scar contrasted to previous studies that reported higher pH values in running waters following forest fires (Earl & Blinn, 2003; Stephens *et al.*, 2004; Badia & Marti, 2008; Hall & Lombardozzi, 2008; Oliver *et al.*, 2012). Wood ash is alkaline and can increase stream water pH by up to 3 pH units (Smith *et al.*, 2011). The lower pH values were associated with periods of very high turbidity when large quantities of black carbon were present in the MRG suggesting a biological or chemical control on pH.

The number and intensity of DO sags downstream of the Las Conchas fire were unexpected. Multiple years of data before the fire provided a strong baseline with which to compare conditions in July and August 2011 immediately after the Las Conchas fire (Fig. 4). Decreases in DO after fire or ash inputs have been observed in other studies using discrete samples of stream water (Earl & Blinn, 2003; Hall & Lombardozzi, 2008); however, continuous measurements of WQ were critical for documenting the severity and duration of effects. Typical grab sampling would miss most of these events. Co-location of sondes with discharge gauges also allows characteristics of discharge events to be linked with WQ. For example, peaks in discharge from runoff from the burn scar of the Las Conchas fire preceded the minimum in DO by up to 8–10 h (Fig. 5). The mechanism creating this offset between the leading edge of flow and DO responses deserves further study and may be linked to the timing of the movement of POC (particulate organic carbon) and DOC (dissolved organic carbon) relative to the flow pulse (Fig. 3f)(Newbold *et al.*, 1997; Thomas *et al.*, 2001).

Mechanisms generating DO sags

Two likely pathways could produce the major DO sags associated with pulses of fire residue. These pathways are intensified chemical oxygen demand (COD) and/or biological oxygen demand (BOD). Sources of COD that might be associated with fire debris include sulphides and reduced metals (e.g. ferrous iron and manganous manganese). Chemically reduced solutes could react with DO and decrease DO concentrations. Data on sulphide concentrations and reduced metals were not collected in the residues of the moderately and severely burned zones after the Las Conchas fire, so it is difficult to assess the importance of chemical pathways in removing DO from solution. Reducing conditions where large quantities of ash and charcoal were produced by high-temperature fire may be sources of COD to the river network, but the importance of such pathways in generating strong DO sags requires further research.

The second pathway (BOD) that could generate large DO sags is microbial metabolism of organic matter (Reid, Thoms & Dyer, 2006; Marañón-Jiménez *et al.*, 2013). Large quantities of partially oxidised organic matter are produced by intense wildfire, and these organic materials both decompose within the burn scar and can be washed into the river network (Kim *et al.*, 2004; Hockaday *et al.*, 2007). Aerobic decomposition of both DOC and POC removes DO from water. If concentrations of DOC and POC that are readily decomposed through microbial pathways are high, BOD could generate the strong sags of DO that we measured (Whitworth, Baldwin & Kerr, 2012; Kerr, Baldwin & Whitworth, 2013). Concentrations of DOC and POC were not measured during the pulses of burn scar materials. Measurement of pH by the sondes, however, provides evidence for enhanced metabolism during the fire scar pulses. Aerobic metabolism produces carbon dioxide during microbial respiration that would reduce pH (Stelzer, Heffernan & Likens, 2003; Reid *et al.*, 2006). The concurrent pH sags, which were not observed in other studies (Earl & Blinn, 2003; Hall & Lombardozzi, 2008; Smith *et al.*, 2011), with DO sags when high turbidity conditions occurred at the sonde sites suggest a role for BOD in producing at least some of the measured DO depletions, although COD pathways too can reduce pH values.

Black carbon is produced from incomplete combustion of organic matter in the absence of oxygen (Shrestha, Traina & Swanston, 2010). Wildfires are an important mechanism for the formation of black carbon via the smouldering combustion of wood and the litter layer. The oxidation and degradation of black carbon are not yet well understood (Shrestha *et al.*, 2010), but microbial pathways (BOD) are likely to be primary drivers of decomposition (Nguyen & Lehmann, 2009). The generation of DOC from charcoal and other forms of black carbon also produces a potential soluble source of organic matter for microbial metabolism (Hockaday *et al.*, 2007). Large quantities of black carbon were mobilised during the initial flow events from the Las Conchas burn scar (Fig. 3), and we hypothesise that the organic matter from black carbon residues, both POC and DOC, played an important role in the dramatic DO sags in the Rio Grande in July and August 2011. Clearly, further research is needed on the biodegradability of black carbon derived from forest fires and potential links between DO sags, enhanced BOD and pH sags in streams and rivers receiving runoff from fire scars.

Radar and flash floods

Determining the location and intensity of rainfall events that produce flash floods off burn scars assist in evaluating source areas for black carbon in a river network, the network connections transporting these materials and the timing of flood waters reaching downstream points. Combining NEXRAD data analyses, continuous *in situ* sensor monitoring and continuous discharge measurements provides tools to track the propagation of a WQ disturbance from the source throughout a river network.

Broader implications

Increased wildfire activity in the western United States has already been documented (Westerling *et al.*, 2006). This is due to atmospheric warming and earlier spring conditions that produce a higher frequency of fires, longer duration fires and a longer fire season. Post-fire tree mortality also is increasing along with higher fire severity (Van Mantgem *et al.*, 2013). These stresses on forests with accelerated tree mortality due to drought and heat are found worldwide (Allen *et al.*, 2010). Conditions conducive to larger and more severe forest fires are increasing worldwide, and WQ impacts such as were seen immediately after the Las Conchas fire are likely to become more prevalent. Hypoxia and anoxia, transport of large quantities of black carbon and exceptionally high turbidities are by-products of flash floods flowing off large and severely burned landscapes.

Major disturbances that load large amounts of organic matter into aquatic ecosystems often strongly deplete DO. Catastrophic forest fires are clear examples of a disturbance with potential for large-scale organic matter loading when precipitation events transport black carbon into river networks. Another example of a major disturbance that can load large quantities of organic matter into aquatic ecosystems is a volcanic eruption. The eruption of Mount St. Helens in May of 1980 loaded large quantities of organic carbon from the devastated forest into about 20 lakes in the blast zone. These lakes were highly enriched in both DOC and POC and became hypoxic or anoxic during the summer months after the eruption, with extremely large increases in bacterial numbers and activity (Baross *et al.*, 1982; Wissmar *et al.*, 1982; Dahm *et al.*, 1983; Lilley, Baross & Dahm, 1988). Some of the most impacted lakes had no measureable DO from just below the surface to the bottom throughout August 1980.

Another example where hypoxia and anoxia were induced by the interaction between large quantities of organic matter with flowing water was the reintroduction of the flood pulse to a river floodplain that had been isolated from the river for decades (Valett *et al.*, 2005). Very high rates of metabolism quickly removed the DO from the flood waters and anaerobic pathways of decomposition became prevalent. Disturbances that connect terrestrial environments rich in organic carbon with aquatic ecosystems facilitate microbial metabolism of these energy resources and can draw down DO concentrations rapidly.

A final example of a large-scale disturbance that produced major WQ changes to river ecosystems similar to those we measured occurred in the southern Murray-Darling Basin in Australia in the spring and summer of 2010-2011 (Hladyz *et al.*, 2011; Whitworth *et al.*, 2012; Kerr *et al.*, 2013). Flooding after more than a decade of drought inundated forested and agricultural floodplains and produced hypoxic blackwater events (DO < 2 mg L^{-1} combined with high DOC) over 2000 km of river channel for up to 6 months. Such hypoxic blackwater events can be enhanced by higher temperatures and human regulation of the hydrograph. The flooding of long-isolated floodplains mobilised bioavailable DOC that stimulated microbial activity that lowered DO concentrations, commonly to below 2 mg L^{-1}.

The important role of DOC in producing hypoxia in these rivers after the breaking of long-term drought argues for the need to measure concentrations and bioavailability of DOC in stream and river water after catastrophic forest fires. Kerr *et al.* (2013) presented a flow chart that summarises the processes leading to hypoxic blackwater. The processes were the accumulation of organic matter on the floodplain, floodplain inundation, DOC release, BOD and COD exceeding re-oxygenation rates and DO-depleted river water. These steps work well to explain the generation of hypoxia and anoxia after high-intensity forest fires where the organic matter is black carbon from incomplete combustion and flash floods transport organic matter to streams and rivers and release DOC into solution (Fig. 3). Increasingly, severe forest fires and longer warmer periods of drought are predicted for many regions worldwide in the coming

© 2015 John Wiley & Sons Ltd,

decades, and the impacts of these changes on WQ deserve further attention.

Acknowledgments

The authors thank their colleagues in the Hydrogeoecology Group at the University of New Mexico, past and present, for their ideas and guidance and for their assistance in the field and in the laboratory. We also want to give special thanks to Dr. Robert R. Parmenter, Director of Science and Education at the Valles Caldera National Preserve, Todd Kelly and Daniel Blankenship, USGS New Mexico Water Science Centre, the Albuquerque Metropolitan Arroyo Flood Control Authority and Phoebe Suina, Cochiti Pueblo, for their information and photographs concerning storms mobilising and transporting fire scar material in the time immediately after the Las Conchas fire. We thank Dave Strayer, Mark Ledger and two anonymous reviewers for their assistance in improving this manuscript. We acknowledge the U.S. Army Corps of Engineers, Albuquerque District, the U.S. National Science Foundation through the New Mexico Experimental Program to Stimulate Competitive Research (NM EPSCoR) and the Long-Term Ecological Research (LTER) Program for funding of this research. This is publication number SEV 700 from the Sevilleta LTER Project.

References

Allen C.D. (2001) Fire and vegetation history of the Jemez Mountains. In: *Water, Watersheds, and Land Use In New Mexico: Impacts of Population Growth on Natural Resources, Santa Fe Region 2001*. (Ed P.S. Johnson), pp. 29–33. New Mexico Bureau of Mines and Mineral Resources, Socorro, NM.

Allen C.D., Macalady A.K., Chenchouni H., Bachelet D., McDowell N., Vennetier M. *et al.* (2010) A global overview of drought and heat-induced tree mortality reveals emerging climate change risks for forests. *Forest Ecology and Management*, **259**, 660–684.

Badia D. & Marti C. (2008) Fire and rainfall energy effects on soil erosion and runoff generation in semi-arid forested lands. *Arid Land Research and Management*, **22**, 93–108.

Baross J.A., Dahm C.N., Ward A.K., Lilley M.D. & Sedell J.R. (1982) Initial microbiological response in lakes to the Mount St. Helens eruption. *Nature*, **296**, 49–52.

Bestgen K.R. & Platania S.P. (1991) Status and conservation of the Rio Grande Silvery Minnow, *Hybognathus amarus*. *Southwestern Naturalist*, **36**, 225–232.

Dahm C.N., Baross J.A., Ward A.K., Lilley M.D. & Sedell J.R. (1983) Initial effects of the Mount St. Helens eruption on nitrogen cycle and related chemical processes in Ryan Lake. *Applied and Environmental Microbiology*, **45**, 1633–1645.

Dahm C.N., Cleverly J.R., Coonrod J.E.A., Thibault J.R., McDonnell D.E. & Gilroy D.F. (2002) Evapotranspiration at the land/water interface in a semi-arid drainage basin. *Freshwater Biology*, **47**, 831–843.

DeBano L.F. (1981) *Water Repellent Soils: A state-of-the-art*, General Technical Report PSW-46, US Department of Agriculture, Forest Service, Pacific Southwest Forest and Range Experiment Station, Berkeley, CA, 21 pp.

DeBano L.F. (2000) The role of fire and soil heating on water repellency in wildland environments: a review. *Journal of Hydrology*, **231–232**, 195–206.

Dudley R.K. & Platania S.P. (2007) Flow regulation and fragmentation imperil pelagic-spawning riverine fishes. *Ecological Applications*, **17**, 2074–2086.

Earl S.R. & Blinn D.W. (2003) Effects of wildfire ash on water chemistry and biota in South-Western USA streams. *Freshwater Biology*, **48**, 1015–1030.

Gresswell R.E. (1999) Fire and aquatic ecosystems in forested biomes of North America. *Transactions of the American Fisheries Society*, **128**, 193–221.

Gutzler D.S. (2013) Regional climatic considerations for borderlands sustainability. *Ecosphere*, **4**, Article 7.

Hall S.J. & Lombardozzi D. (2008) Short-term effects of wildfire on montane stream ecosystems in southern Rocky Mountains: one and two years post-burn. *Western North American Naturalist*, **68**, 453–462.

Hladyz S., Watkins S.C., Whitworth K.L. & Baldwin D.S. (2011) Flows and hypoxic blackwater events in managed ephemeral river channels. *Journal of Hydrology*, **401**, 117–125.

Hockaday W.C., Grannas A.M., Kim S. & Hatcher P.G. (2007) The transformation and mobility of charcoal in a fire-impacted watershed. *Geochimica et Cosmochimica Acta*, **71**, 3432–3445.

Kerr J.L., Baldwin D.S. & Whitworth K.L. (2013) Options for managing hypoxic blackwater events in river systems: a review. *Journal of Environmental Management*, **114**, 139–147.

Kim S., Kaplan L.A., Benner R. & Hatcher P.G. (2004) Hydrogen-deficient molecules in natural riverine water samples—evidence for the existence of black carbon in DOM. *Marine Chemistry*, **92**, 225–234.

Knowles N., Dettinger M.D. & Cayan D.R. (2006) Trends in snowfall versus rainfall in the western United States. *Journal of Climate*, **19**, 4545–4559.

Lavine A., Kuyumjian G.A., Reneau S.L., Katzman D. & Malmon D.V. (2006) A five-year record of sedimentation in the Los Alamos reservoir, New Mexico, following the Cerro Grande Fire. In: *Joint 8th Federal Interagency Sedimentation Conference and 3rd Federal Interagency Hydrologic Modeling Conference, April 2-6, 2006, Reno, Nevada, USA*. (Ed J.M. Bernard), pp. 951–959. U.S. Geological Survey, Reston, Virginia.

© 2015 John Wiley & Sons Ltd, *Freshwater Biology*, doi: 10.1111/fwb.12548

Lilley M.D., Baross J.A. & Dahm C.N. (1988) Methane production and oxidation in lakes impacted by the May 18, 1980 eruption of Mount St. Helens. *Global Biogeochemical Cycles*, **2**, 357–370.

Malmon D.V., Reneau S.L., Katzman D., Lavine A. & Lyman J. (2007) Suspended sediment transport in an ephemeral stream following wildfire. *Journal of Geophysical Research-Earth Surface*, **112**, F02006.

Marañón-Jiménez S., Castro J., Fernández-Ondoño E. & Zamora R. (2013) Charred wood remaining after a wildfire as a reservoir of macro-and micronutrients in a Mediterranean pine forest. *International Journal of Wildland Fire*, **22**, 681–695.

Molles M.C., Crawford C.S., Ellis L.M., Valett H.M. & Dahm C.N. (1998) Managed flooding for riparian ecosystem restoration. *BioScience*, **48**, 749–756.

Molles M.C. & Dahm C.N. (1990) A perspective on El Niño and La Niña: global implications for stream ecology. *Journal of the North American Benthological Society*, **9**, 68–76.

Newbold J.D., Bott T.L., Kaplan L.A., Sweeney B.W. & Vannote R.L. (1997) Organic matter dynamics in White Clay Creek, Pennsylvania, USA. *Journal of the North American Benthological Society*, **16**, 46–50.

Nguyen B.T. & Lehmann J. (2009) Black carbon decomposition under varying water regimes. *Organic Geochemistry*, **40**, 846–853.

Oliver A.A., Reuter J.E., Heyvaert A.C. & Dahlgren R.A. (2012) Water quality response to the Angora Fire, Lake Tahoe, California. *Biogeochemistry*, **111**, 361–376.

Pelletier J.D. & Orem C.A. (2014) How do sediment yields from post-wildfire debris-laden flows depend on terrain slope, soil burn severity class, and drainage basin area? Insights from airborn-LiDAR change detection. *Earth Surface Processes and Landforms*, **39**, 1822–1832.

Reid M.A., Thoms M.C. & Dyer F.J. (2006) Effects of spatial and temporal variation in hydraulic conditions on metabolism in cobble biofilm communities in an Australian upland stream. *Journal of the North American Benthological Society*, **25**, 756–767.

Seager R., Ting M.F., Held I., Kushnir Y., Lu J., Vecchi G. *et al.* (2007) Model projections of an imminent transition to a more arid climate in southwestern North America. *Science*, **316**, 1181–1184.

Seager R., Tzanova A. & Nakamura J. (2009) Drought in the southeastern United States: causes, variability over the last millennium, and the potential for future hydroclimate change. *Journal of Climate*, **22**, 5021–5045.

Shakesby R.A. & Doerr S.H. (2006) Wildfire as a hydrological and geomorphological agent. *Earth-Science Reviews*, **74**, 269–307.

Sheppard P.R., Comrie A.C., Packin G.D., Angersbach K. & Hughes M.K. (2002) The climate of the US Southwest. *Climate Research*, **21**, 219–238.

Shrestha G., Traina S.J. & Swanston C.W. (2010) Black carbon's properties and role in the environment: a comprehensive review. *Sustainability*, **2**, 294–320.

Smith H.G., Sheridan G.J., Lane P.N., Nyman P. & Haydon S. (2011) Wildfire effects on water quality in forest catchments: a review with implications for water supply. *Journal of Hydrology*, **396**, 170–192.

Stelzer R.S., Heffernan J. & Likens G.E. (2003) The influence of dissolved nutrients and particulate organic matter quality on microbial respiration and biomass in a forest stream. *Freshwater Biology*, **48**, 1925–1937.

Stephens S.L., Meixner T., Poth M., McGurk B. & Payne D. (2004) Prescribed fire, soils, and stream water chemistry in a watershed in the Lake Tahoe Basin, California. *International Journal of Wildland Fire*, **13**, 27–35.

Thomas S.A., Newbold J.D., Monaghan M.T., Minshall G.W., Georgian T. & Cushing C.E. (2001) The influence of particle size on seston deposition in streams. *Limnology and Oceanography*, **46**, 1415–1424.

Touchan R., Woodhouse C.A., Meko D.M. & Allen C.D. (2011) Millennial precipitation reconstruction for the Jemez Mountains, New Mexico, reveals changing drought signal. *International Journal of Climatology*, **31**, 896–906.

Turner T.F. & Edwards M.S. (2012) Aquatic foodweb structure of the Rio Grande assessed with stable isotopes. *Freshwater Science*, **31**, 825–834.

U.S. Army Corps of Engineers (2012) Technical assistance report for Pueble de Cochiti, Las Conchas fire response, Peralta Creek flood mitigation measures., p. 87. Albuquerque District Office, Albuquerque, New Mexico.

Valett H.M., Baker M.A., Morrice J.A., Crawford C.S., Molles M.C., Dahm C.N. *et al.* (2005) Biogeochemical and metabolic responses to the flood pulse in a semiarid floodplain. *Ecology*, **86**, 220–234.

Van Mantgem P.J., Nesmith J.C.B., Keifer M., Knapp E.E., Flint A. & Flint L. (2013) Climatic stress increases forest fire severity across the western United States. *Ecology Letters*, **16**, 1151–1156.

Van Mantgem P.J., Stephenson N.L., Byrne J.C., Daniels L.D., Franklin J.F., Fulé P.Z. *et al.* (2009) Widespread increase of tree mortality rates in the western United States. *Science*, **323**, 521–524.

Veenhuis J.E. (2002) *Effects of wildfire on the hydrology of Capulin and Rito de los Frijoles Canyons, Bandelier National Monument, New Mexico*, US Department of the Interior, US Geological Survey, Water-Resources Investigations Report 02–4152, 39 pp.

Verkaik I., Rieradevall M., Cooper S.D., Melack J.M., Dudley T.L. & Prat N. (2013) Fire as a disturbance in mediterranean climate streams. *Hydrobiologia*, **719**, 353–382.

Wagner R.J., Mattraw H.C., Ritz G.F. & Smith B.A. (2006) *Guidelines and standard procedures for continuous water-quality monitors: Site selection, field operation, calibration, record computation, and reporting*, US Department of the Interior, US Geological Survey Techniques and Methods 1–D3, 51 p. + 8 attachments.

Walsh R.P.D., Boakes D., Coelho C.O.A., Goncalves A.J.B., Shakesby R.A. & Thomas A.D. (1994) Impact of fire-induced hydrophobicity and postfire forest litter on overland flow in northern and central Portugal. In *Second International Conference on Forest Fire Research*. (Viagas D.X. ed). Associacao para o Desenvolvimento da Aerodinamica Industrial, Coimbra, Portugal, pp. 1149–1160.

Westerling A.L., Hidalgo H.G., Cayan D.R. & Swetnam T.W. (2006) Warming and earlier spring increase western US forest wildfire activity. *Science*, **313**, 940–943.

Whitworth K.L., Baldwin D.S. & Kerr J.L. (2012) Drought, floods and water quality: drivers of a severe hypoxic blackwater event in a major river system (the southern Murray-Darling Basin, Australia). *Journal of Hydrology*, **450–451**, 190–198.

Williams A.P., Allen C.D., Macalady A.K., Griffin D., Woodhouse C.A., Meko D.M. *et al*. (2012) Temperature as a potent driver of regional forest drought stress and tree mortality. *Nature Climate Change*, **3**, 292–297.

Wissmar R.C., Devol A.H., Nevissi A.E. & Sedell J.R. (1982) Chemical-changes of lakes within the Mt. St. Helens blast zone. *Science*, **216**, 175–178.

Supporting Information

Additional Supporting Information may be found in the online version of this article:

Fig S1. Water quality parameters (temperature, turbidity, dissolved oxygen, specific conductance and pH) and discharge measured at the USGS water quality station located at the Cochiti Reservoir outfall from July - August, 2011. Note the discharge, turbidity, and specific conductance increases and the dissolved oxygen and pH decreases in late August.

(Manuscript accepted 26 January 2015)